6

Global Characterisation of Constrained Linear Quadratic Optimal Control

6.1 Overview

As stated earlier, a common strategy in applications of receding horizon optimal control is to compute the optimal input u_k at time k by solving, on line, the associated finite horizon optimisation problem. As explained in Chapter 4, when the system and objective function are time-invariant, then this procedure implicitly defines a time-invariant control policy $\mathcal{K}_N : \mathbb{X} \to \mathbb{U}$ of the form $\mathcal{K}_N(x) = u_0^{\text{OPT}}$ (see (4.10) of Chapter 4).

This leads to the obvious question: "Should we repeat the calculation of $\mathcal{K}_N(x)$ in the event that x returns to a value that has been previously visited?" Heuristically, one would immediately answer "No!" to this question. However, a little more thought reveals that to make this a feasible proposition in practice, we need to solve three problems; namely,

(i) how to efficiently calculate $\mathcal{K}_N(x)$ for all x of interest;
(ii) how to store $\mathcal{K}_N(x)$ as a function of x;
(iii) how to retrieve the value of $\mathcal{K}_N(x)$ given x.

In a general setting, these problems present substantial difficulties. However, for the case of constrained linear systems, there exists a relatively simple *finitely parameterised* characterisation of $\mathcal{K}_N(x)$, which can be computed and stored efficiently for *small* state dimensions and *short* horizons. We present this characterisation in this chapter, leading to an explicit form for the receding horizon control policy. Even if, on the balance of computational time, one decides to still solve the quadratic programming [QP] problem at each step, we believe that this finitely parameterised characterisation of $\mathcal{K}_N(x)$ gives practically valuable insights into the nature of the constrained control policy.

We first derive the characterisation using dynamic programming (introduced in Section 3.4 of Chapter 3). We consider systems with a single input constrained to lie in an interval and optimisation horizon $N = 2$. We then analyse the geometric structure of the fixed horizon optimal control problem $\mathcal{P}_N$ when seen as a QP of the form discussed in Section 5.3 of Chapter 5.

Using this geometric structure, we will re-derive the result obtained via dynamic programming. This will give insight into the solution by clarifying the interrelationship between dynamic programming and the inherent geometry of the QP solution space (the space where the QP is defined).

We then show how the same ideas can be used to characterise the solution of the fixed horizon optimal control problem $\mathcal{P}_N$ for cases with arbitrary horizons and more general linear constraints. As for the simpler case $N = 2$, the general solution is obtained by exploiting the geometry of the associated QP in particular coordinates of its solution space. Once projected onto the state space, the result is a *piecewise affine* characterisation, that is, a partition of the state space into regions in which the corresponding control law is affine.

Finally, we discuss the use of the KKT optimality conditions (Sections 2.5.4–2.5.5 in Chapter 2) in the derivation of the piecewise affine characterisation.

6.2 Global Characterisation for Horizon 2 via Dynamic Programming

For ease of exposition, here we will fix the optimisation horizon to $N = 2$.

We consider single input, linear, discrete time systems in which the magnitude of the control input is constrained to be less than or equal to a positive constant. In particular, let the system be given by

$$x_{k+1} = Ax_k + Bu_k, \qquad |u_k| \leq \Delta, \tag{6.1}$$

where $x_k \in \mathbb{R}^n$ and $\Delta > 0$ is the input constraint level. Consider the following fixed horizon optimal control problem

$$\begin{aligned} \mathcal{P}_2(x): \qquad & V_2^{\mathrm{OPT}}(x) \triangleq \min V_2(\{x_k\}, \{u_k\}), \\ & \text{subject to:} \\ & x_{k+1} = Ax_k + Bu_k \quad \text{for } k = 0, 1, \\ & x_0 = x, \\ & u_k \in \mathbb{U} \triangleq [-\Delta, \Delta] \quad \text{for } k = 0, 1, \end{aligned} \tag{6.2}$$

where the objective function in (6.2) is

$$V_2(\{x_k\}, \{u_k\}) \triangleq \frac{1}{2} x_2^{\mathrm{T}} P x_2 + \frac{1}{2} \sum_{k=0}^{1} \left(x_k^{\mathrm{T}} Q x_k + u_k^{\mathrm{T}} R u_k \right). \tag{6.3}$$

The matrices Q and R in (6.3) are positive definite and P satisfies the algebraic Riccati equation

$$P = A^{\mathrm{T}} P A + Q - K^{\mathrm{T}} \bar{R} K, \tag{6.4}$$

where

$$K \triangleq \bar{R}^{-1} B^{\mathrm{T}} P A, \qquad \bar{R} \triangleq R + B^{\mathrm{T}} P B. \tag{6.5}$$

Let the control sequence that minimises (6.3) be

$$\{u_0^{\mathrm{OPT}}, u_1^{\mathrm{OPT}}\}. \tag{6.6}$$

Then the RHC law is given by the first element of (6.6) (which depends on the current state $x_0 = x$), that is,

$$\mathcal{K}_2(x) = u_0^{\mathrm{OPT}}. \tag{6.7}$$

Before proceeding with the solution to the above problem, we observe that, at this stage, the choice of the matrix P as the solution to (6.4) is not necessary; however, as we showed in Chapter 5, this choice is useful to establish stability of the receding horizon implementation given by the state equation in (6.1) in closed loop with $u_k = \mathcal{K}_2(x_k)$. Also, this choice effectively gives an infinite horizon objective function with the restriction that constraints not be active after the first two steps. Similarly, the assumption that Q is positive definite is not required at this stage, but it will be used later in the stability result of Section 7.2.2 in the following chapter.

In Theorem 6.2.1 below, we will derive the solution of $\mathcal{P}_2$ defined in (6.2)–(6.5) using dynamic programming. Following Section 3.4 of Chapter 3, the partial value functions at each step of the dynamic programming algorithm, are defined by

$$V_0^{\mathrm{OPT}}(x_2) \triangleq \frac{1}{2} x_2^{\mathrm{T}} P x_2, \tag{6.8}$$

$$V_1^{\mathrm{OPT}}(x_1) \triangleq \min_{\substack{u_1 \in \mathbb{U} \\ x_2 = A x_1 + B u_1}} \frac{1}{2} x_2^{\mathrm{T}} P x_2 + \frac{1}{2} x_1^{\mathrm{T}} Q x_1 + \frac{1}{2} u_1^{\mathrm{T}} R u_1,$$

and $V_2^{\mathrm{OPT}}(x)$ is the value function of $\mathcal{P}_2$ defined in (6.2)–(6.3).

The dynamic programming algorithm makes use of the principle of optimality, which states that any portion of the optimal trajectory is itself an optimal trajectory. That is, for $k = 0, 1$, (see (3.85) in Chapter 3)

$$V_k^{\mathrm{OPT}}(x) = \min_{u \in \mathbb{U}} \frac{1}{2} x^{\mathrm{T}} Q x + \frac{1}{2} u^{\mathrm{T}} R u + V_{k-1}^{\mathrm{OPT}}(Ax + Bu), \tag{6.9}$$

where u and x denote, $u = u_k$ and $x = x_k$, respectively.

In the sequel we will use the saturation function $\mathrm{sat}_\Delta(\cdot)$ defined, for the saturation level Δ, as

$$\mathrm{sat}_\Delta(u) \triangleq \begin{cases} \Delta & \text{if } u > \Delta, \\ u & \text{if } |u| \leq \Delta, \\ -\Delta & \text{if } u < -\Delta. \end{cases} \tag{6.10}$$

The following result gives a finitely parameterised characterisation of the RHC law (6.7).

Theorem 6.2.1 (RHC Characterisation for N = 2) *The RHC law* (6.7) *has the form*

$$\mathcal{K}_2(x) = \begin{cases} -\mathrm{sat}_\Delta(Gx+h) & \text{if } x \in \mathbb{Z}^-, \\ -\mathrm{sat}_\Delta(Kx) & \text{if } x \in \mathbb{Z}, \\ -\mathrm{sat}_\Delta(Gx-h) & \text{if } x \in \mathbb{Z}^+, \end{cases} \tag{6.11}$$

where K is given by (6.5)*, the gain $G \in \mathbb{R}^{1\times n}$ and the constant $h \in \mathbb{R}$ are given by*

$$G \triangleq \frac{K + KBKA}{1+(KB)^2}, \qquad h \triangleq \frac{KB}{1+(KB)^2}\Delta, \tag{6.12}$$

and the sets $(\mathbb{Z}^-, \mathbb{Z}, \mathbb{Z}^+)$ are defined by

$$\mathbb{Z}^- \triangleq \{x : K(A-BK)x < -\Delta\}, \tag{6.13}$$

$$\mathbb{Z} \triangleq \{x : |K(A-BK)x| \le \Delta\}, \tag{6.14}$$

$$\mathbb{Z}^+ \triangleq \{x : K(A-BK)x > \Delta\}. \tag{6.15}$$

Proof. We start from the last partial value function (6.8), at time $k = N = 2$, and solve the problem backwards in time using (6.9).

(i) The partial value function V_0^{OPT} $(k = N = 2)$:
Here $x = x_2$. By definition, the partial value function at time $k = N = 2$ is

$$V_0^{\mathrm{OPT}}(x) \triangleq \frac{1}{2}x^{\mathrm{T}}Px \quad \text{for all } x \in \mathbb{R}^n.$$

(ii) The partial value function V_1^{OPT} $(k = N-1 = 1)$:
Here $x = x_1$ and $u = u_1$. By the principle of optimality, for all $x \in \mathbb{R}^n$,

$$\begin{aligned} V_1^{\mathrm{OPT}}(x) &= \min_{u\in\mathbb{U}} \left\{ \frac{1}{2}x^{\mathrm{T}}Qx + \frac{1}{2}u^{\mathrm{T}}Ru + V_0^{\mathrm{OPT}}(Ax+Bu) \right\} \\ &= \min_{u\in\mathbb{U}} \left\{ \frac{1}{2}x^{\mathrm{T}}Qx + \frac{1}{2}u^{\mathrm{T}}Ru + \frac{1}{2}(Ax+Bu)^{\mathrm{T}}P(Ax+Bu) \right\} \\ &= \min_{u\in\mathbb{U}} \left\{ \frac{1}{2}x^{\mathrm{T}}Px + \frac{1}{2}\bar{R}(u+Kx)^2 \right\}, \end{aligned} \tag{6.16}$$

where $\bar{R}$ is defined in (6.5). In deriving (6.16) we have made use of (6.4). It is clear that the *unconstrained* $(u \in \mathbb{R})$ optimal control is given by $u = -Kx$. From the convexity of the function $\bar{R}(u+Kx)^2$ it then follows that the *constrained* $(u \in \mathbb{U})$ optimal control law, which corresponds to the second element of the sequence (6.6), is given by

$$u_1^{\mathrm{OPT}} = \mathrm{sat}_\Delta(-Kx) = -\mathrm{sat}_\Delta(Kx) \quad \text{for all } x \in \mathbb{R}^n, \tag{6.17}$$

and the partial value function at time $k = N-1 = 1$ is

$$V_1^{\mathrm{OPT}}(x) = \frac{1}{2}x^{\mathrm{T}}Px + \frac{1}{2}\bar{R}\left[Kx - \mathrm{sat}_\Delta(Kx)\right]^2 \quad \text{for all } x \in \mathbb{R}^n.$$

(iii) The (partial) value function V_2^{OPT} ($k = N - 2 = 0$):
Here $x = x_0$ and $u = u_0$. By the principle of optimality, we have that, for all $x \in \mathbb{R}^n$,

$$\begin{aligned} V_2^{\mathrm{OPT}}(x) &= \min_{u\in\mathbb{U}} \left\{ \frac{1}{2}x^{\mathrm{T}}Qx + \frac{1}{2}u^{\mathrm{T}}Ru + V_1^{\mathrm{OPT}}(Ax+Bu) \right\} \\ &= \min_{u\in\mathbb{U}} \left\{ \frac{1}{2}x^{\mathrm{T}}Qx + \frac{1}{2}u^{\mathrm{T}}Ru + \frac{1}{2}(Ax+Bu)^{\mathrm{T}}P(Ax+Bu) \right. \\ &\quad \left. + \frac{1}{2}\bar{R}\left[K(Ax+Bu) - \mathrm{sat}_\Delta(K(Ax+Bu))\right]^2 \right\} \\ &= \frac{1}{2}\min_{u\in\mathbb{U}} \Big\{ x^{\mathrm{T}}Px + \bar{R}(u+Kx)^2 \\ &\quad + \bar{R}\left[KAx + KBu - \mathrm{sat}_\Delta(KAx+KBu)\right]^2 \Big\}. \end{aligned} \tag{6.18}$$

Denote the terms in (6.18) by $f_1(u) \triangleq (u+Kx)^2$, and $f_2(u) \triangleq [KAx + KBu - \mathrm{sat}_\Delta(KAx+KBu)]^2$. Notice that the function $f_2(u)$ has a "cup" shape formed by three zones: (a) Half-parabola corresponding to the case $KAx + KBu < -\Delta$; (b) a flat zone corresponding to the case $|KAx + KBu| \leq \Delta$, and; (c) half-parabola corresponding to the case $KAx + KBu > \Delta$. Note also that $f_1 + f_2$ is convex. With this information, we can derive the result (6.11) as follows:

Case (a). $x \in \mathbb{Z}^-$: In this case, the minimiser of $f_1(u)$ (that is, $u = -Kx$) is such that $KAx + KB(-Kx) = K(A - BK)x < -\Delta$ (see (6.13)), that is, $u = -Kx$ is in zone (a) of function $f_2(u)$. Then, the minimum of $f_1(u)+f_2(u)$ (situated between the minimum of $f_1(u)$, at $u = -Kx$, and the minimum of $f_2(u)$) will also fall in zone (a). We conclude that the value function is

$$V_2^{\mathrm{OPT}}(x) = \frac{1}{2}\min_{u\in\mathbb{U}} \left\{ x^{\mathrm{T}}Px + \bar{R}(u+Kx)^2 + \bar{R}\left[KAx + KBu + \Delta\right]^2 \right\},$$

whose unconstrained minimum is easily found to be at $u = -(Gx+h)$, with G and h as given in (6.12). From the convexity of $f_1(u)+f_2(u)$ it then follows that the *constrained* ($u \in \mathbb{U}$) optimal control law, which corresponds to the first element of the sequence (6.6), is given by

$$u_0^{\mathrm{OPT}} = -\mathrm{sat}_\Delta(Gx+h) \quad \text{for all } x \in \mathbb{Z}^-.$$

This shows the result in (6.11) for this case.

Case (b). $x \in \mathbb{Z}$: This case corresponds to the situation where $u = -Kx$ is in zone (b) of $f_2(u)$ and hence, the unconstrained minimum of $f_1(u) + f_2(u)$ occurs at $u = -Kx$. Again, using the convexity of $f_1(u)+f_2(u)$, it follows that the *constrained* optimal control law, which corresponds to the first element of the sequence (6.6), is

$$u_0^{\mathrm{OPT}} = -\mathrm{sat}_\Delta(Kx) \quad \text{for all } x \in \mathbb{Z}. \tag{6.19}$$

Case (c). $x \in \mathbb{Z}^+$: The result follows from a similar analysis to the case (a).

□

We illustrate the above result by a simple example.

Example 6.2.1. Consider again the double integrator of Example 1.2.1 in Chapter 1. For this system, we consider an input saturation level $\Delta = 1$.

In the fixed horizon objective function (6.3) we take $Q = \begin{bmatrix} 1 & 0 \\ 0 & 0 \end{bmatrix}$, and $R = 0.1$. The gain K is computed from (6.4)–(6.5). Equation (6.12) gives $G = [-0.6154 \quad -1.2870]$ and $h = 0.4156$.

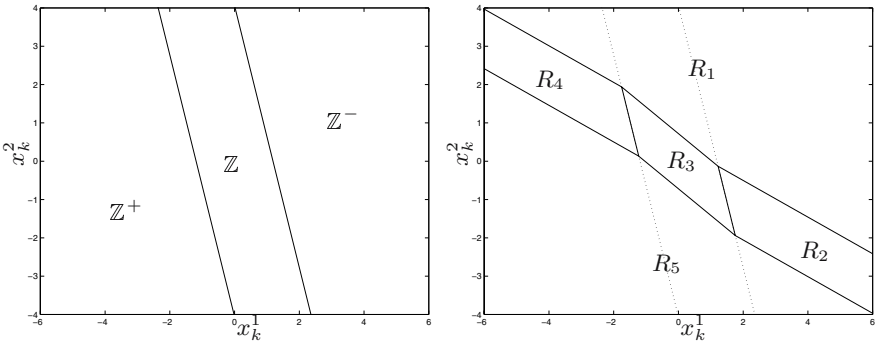

(a) Partition for control law (6.11). (b) Partition for control law (6.20).

Figure 6.1. State space partitions for Example 6.2.1.

In Figure 6.1 (a) we show the sets $\mathbb{Z}^-$, $\mathbb{Z}$ and $\mathbb{Z}^+$ that define the controller (6.11). In this figure, x_k^1 and x_k^2 denote the two components of the state vector x_k.

Actually, we can be even more explicit regarding the form of the control law. In particular, if we discriminate between the regions where each component of the controller (6.11) is saturated from the ones where it is not, we can parameterise the controller (6.11) in the following equivalent, but more explicit, form:

$$\mathcal{K}_2(x) = \begin{cases} -\Delta & \text{if } x \in R_1, \\ -Gx - h & \text{if } x \in R_2, \\ -Kx & \text{if } x \in R_3, \\ -Gx + h & \text{if } x \in R_4, \\ \Delta & \text{if } x \in R_5. \end{cases} \tag{6.20}$$

In Figure 6.1 (b) we show the state space partition that corresponds to the parameterisation (6.20) for this example. ∘

Theorem 6.2.1 shows that the solution to the simple RHC problem (6.2)–(6.7) has the form of a piecewise affine feedback control law defined on a partition of the state space. We will see below that a similar characterisation can be obtained for more general cases. Rather than extending the above procedure, we will utilise alternative geometric arguments.

6.3 The Geometry of Quadratic Programming

As mentioned in Chapter 5, when the system model is linear and the objective function quadratic, the fixed horizon optimal control problem $\mathcal{P}_N$ can be transformed into a QP of the form (5.28). We will start by re-examining the optimal control problem for horizon $N = 2$ defined in (6.2)–(6.5). In this case, the corresponding QP optimal solution is (see (5.29) in Chapter 5 and (6.4)–(6.5))

$$\text{QP:} \qquad \mathbf{u}^{\text{OPT}}(x) = \arg\min_{\mathbf{u}\in R_{\text{UC}}} \frac{1}{2}\mathbf{u}^{\text{T}} H \mathbf{u} + \mathbf{u}^{\text{T}} F x, \tag{6.21}$$

where

$$\mathbf{u} = \begin{bmatrix} u_0 \\ u_1 \end{bmatrix}, \qquad H = \bar{R}\begin{bmatrix} 1+(KB)^2 & KB \\ KB & 1 \end{bmatrix}, \qquad F = \bar{R}\begin{bmatrix} K+KBKA \\ KA \end{bmatrix}, \tag{6.22}$$

and R_{UC} is the square $[-\Delta, \Delta] \times [-\Delta, \Delta] \subset \mathbb{R}^2$. Note that the Hessian H is positive definite since $\bar{R} = R + B^{\text{T}} P B$ is positive because we have assumed that $R > 0$ in (6.3).

The QP in (6.21) has a nice geometric interpretation in the $\mathbf{u}$-space. Consider the equation

$$\frac{1}{2}\mathbf{u}^{\text{T}} H \mathbf{u} + \mathbf{u}^{\text{T}} F x = c, \tag{6.23}$$

where c is a constant. This defines ellipsoids in $\mathbb{R}^2$ centred at $\mathbf{u}_{\text{UC}}^{\text{OPT}}(x) = -H^{-1}Fx$. Then (6.21) can be regarded as the problem of finding the smallest ellipsoid that intersects the boundary of R_{UC}, and $\mathbf{u}^{\text{OPT}}(x)$ is the point of intersection. This is illustrated in Figure 6.2.

The problem can be significantly simplified if we make a coordinate transformation via the square root of the Hessian, that is,

$$\tilde{\mathbf{u}} = H^{1/2}\mathbf{u}. \tag{6.24}$$

In the new coordinates defined by (6.24), the constraint set R_{UC} is mapped into another set, denoted also by R_{UC} for simplicity of notation. The ellipsoids (6.23) take the form of spheres centred at $\tilde{\mathbf{u}}_{\text{UC}}^{\text{OPT}}(x) = -H^{-1/2}Fx$. Thus

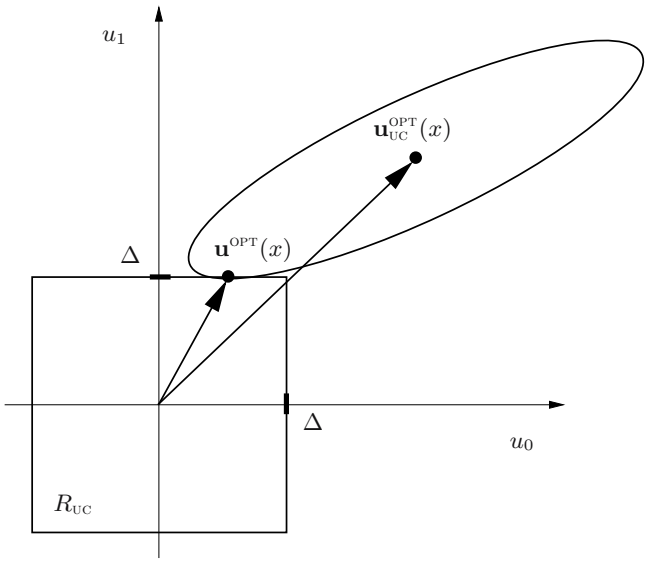

Figure 6.2. Geometric interpretation of QP.

(6.21) is transformed into the problem of finding the point in R_{UC} that is closest to $\tilde{\mathbf{u}}_{\mathrm{UC}}^{\mathrm{OPT}}(x)$ in the Euclidean distance. This is qualitatively illustrated in Figure 6.3.

This transformed geometric picture allows us to immediately write down the solution to the fixed horizon optimal control problem for this special case. In particular, the solution of the QP is obtained by partitioning $\mathbb{R}^2$ into nine regions; the first region is the parallelogram R_{UC}. The remaining regions, denoted by R_1 to R_8, are delimited by lines that are normal to the faces of the parallelogram and pass through its vertices, as shown in Figure 6.3. The optimal constrained solution $\tilde{\mathbf{u}}^{\mathrm{OPT}}(x)$ is determined by the region in which the optimal unconstrained solution $\tilde{\mathbf{u}}_{\mathrm{UC}}^{\mathrm{OPT}}(x)$ lies, in the following way: First, it is clear that $\tilde{\mathbf{u}}^{\mathrm{OPT}}(x) = \tilde{\mathbf{u}}_{\mathrm{UC}}^{\mathrm{OPT}}(x)$ if $\tilde{\mathbf{u}}_{\mathrm{UC}}^{\mathrm{OPT}}(x) \in R_{\mathrm{UC}}$; that is, the optimal constrained solution coincides with the optimal unconstrained solution in R_{UC}. Next, the optimal constrained solution in each of the regions R_1, R_3, R_5 and R_7 is simply equal to the vertex that is contained in the region. Finally, the optimal constrained solution in the regions R_2, R_4, R_6 and R_8 is defined by the orthogonal projection of $\tilde{\mathbf{u}}_{\mathrm{UC}}^{\mathrm{OPT}}(x)$ onto the faces of the parallelogram. This can be seen from Figure 6.3, where a case in which the solution falls in R_8 is illustrated.

Whilst we have concentrated on the simple case $N = 2$, it is easy to see that this methodology can be applied also to more complex cases. Indeed, in Section 6.5 we will apply these geometric arguments to arbitrary horizons and multiple input systems.

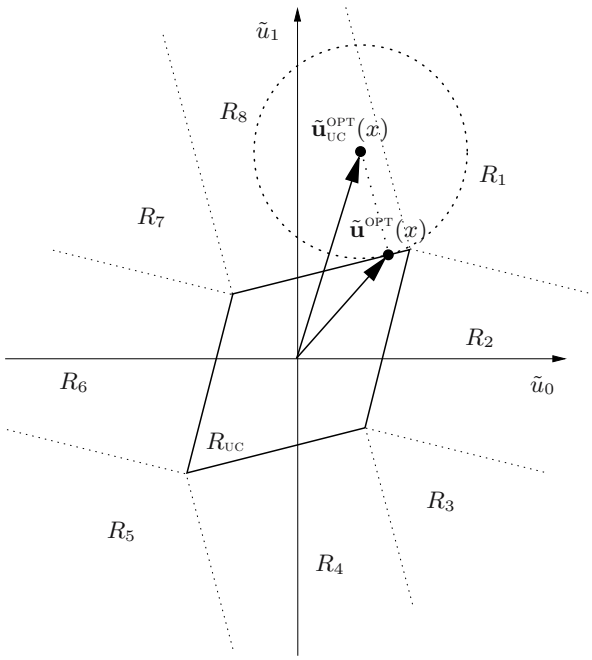

Figure 6.3. Geometry of QP as a minimum Euclidean distance problem.

We thus see that the geometry of the QP problem gives insight into its solution. We will expand on these ideas in the following sections.

6.4 Geometric Characterisation for Horizon 2

In this section, we will use the geometric ideas outlined in Section 6.3 to recover the finitely parameterised characterisation derived via dynamic programming in Theorem 6.2.1.

To solve (6.21), we use the transformation (6.24), which maps the square R_{UC} into the parallelogram R_{UC} shown in Figure 6.3. We next note that the unconstrained solution in the $\tilde{\mathbf{u}}$–coordinates is given by

$$\tilde{\mathbf{u}}_{\mathrm{UC}}^{\mathrm{OPT}}(x) = -H^{-1/2}Fx. \tag{6.25}$$

We then derive the constrained solution in the $\tilde{\mathbf{u}}$–coordinates using geometric arguments, and finally use the transformation

$$\tilde{\mathbf{u}} = -H^{-1/2}Fx \tag{6.26}$$

to retrieve the solution in the state space.

Following Section 6.3, we partition $\mathbb{R}^2$ into nine regions; the first region is the parallelogram $R_{\rm UC}$, and the remaining regions, denoted by R_1 to R_8, are delimited by lines that are normal to the faces of $R_{\rm UC}$ and pass through its vertices, as shown in Figure 6.3.

In $R_{\rm UC}$ we have

$$\tilde{\mathbf{u}}^{\rm OPT}(x) = \tilde{\mathbf{u}}^{\rm OPT}_{\rm UC}(x) = -H^{-1/2}Fx \quad \text{for all } \mathbf{u} \in R_{\rm UC}.$$

That is, in $R_{\rm UC}$ the optimal constrained solution coincides with the optimal unconstrained solution.

To describe the solution in regions R_1 to R_8 in more detail, we introduce the following notation, which will be used in the remainder of the chapter.

Notation 6.4.1 *Given any matrix (column vector) M, and a set of indices $\bar{\ell}$ (with, at most, as many elements as the number of rows of M), the notation $M_{\bar{\ell}}$ identifies the submatrix (subvector) of M formed by selecting the rows with indices given by the elements of $\bar{\ell}$ and all of its columns.* ∘

For example, given H defined in (6.22), and the set $\bar{\ell} = \{2\}$, $H_{\bar{\ell}} = H_2$ denotes its second row.

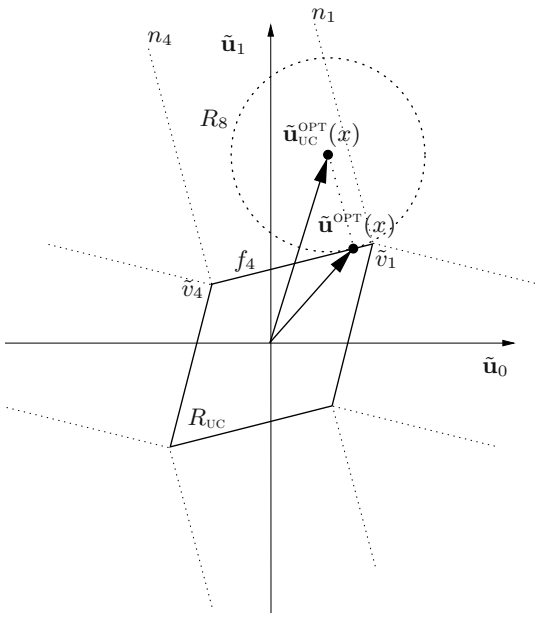

Figure 6.4. Solution of QP in region R_8.

Consider now, for example, region R_8 in Figure 6.4. It is delimited by face f_4 and its normals n_1 and n_4 passing through the vertices $\tilde{v}_1$ and $\tilde{v}_4$,

respectively. The line that contains face f_4 (the line is also denoted by f_4, for simplicity) corresponds to the second control u_1 equal to the saturation level Δ, that is $u_1 = [0 \;\; 1]\mathbf{u} = \Delta$ in the original $\mathbf{u}$-coordinates. In the new $\tilde{\mathbf{u}}$-coordinates (6.24), it is then defined by the equation

$$f_4 : \qquad [0 \;\; 1]H^{-1/2}\tilde{\mathbf{u}} = \Delta. \tag{6.27}$$

Lines normal to f_4 are defined by the equation

$$[1 \;\; 0]H^{1/2}\tilde{\mathbf{u}} = c, \qquad c \in \mathbb{R}. \tag{6.28}$$

Hence, the equation defining n_1 is obtained by setting

$$\tilde{\mathbf{u}} = \tilde{v}_1 = H^{1/2}\Delta[1 \;\; 1]^{\mathrm{T}}$$

in (6.28). This yields

$$n_1 : \qquad [1 \;\; 0]H^{1/2}\tilde{\mathbf{u}} = H_1\Delta[1 \;\; 1]^{\mathrm{T}}. \tag{6.29}$$

In a similar way, the equation defining n_4 is given by

$$n_4 : \qquad [1 \;\; 0]H^{1/2}\tilde{\mathbf{u}} = H_1\Delta[-1 \;\; 1]^{\mathrm{T}}. \tag{6.30}$$

Combining (6.27), (6.29) and (6.30), region R_8 is defined in the $\tilde{\mathbf{u}}$-coordinates by

$$R_8 : \qquad \begin{cases} [0 \;\; 1]H^{-1/2}\tilde{\mathbf{u}} \geq \Delta \\ H_1\Delta[-1 \;\; 1]^{\mathrm{T}} \leq [1 \;\; 0]H^{1/2}\tilde{\mathbf{u}} \leq H_1\Delta[1 \;\; 1]^{\mathrm{T}}, \end{cases} \tag{6.31}$$

and, using the transformation (6.26), it is defined in the state space coordinates $x \in \mathbb{R}^n$ by

$$R_8 : \qquad \begin{cases} -K(A - BK)x \geq \Delta \\ H_1\Delta[-1 \;\; 1]^{\mathrm{T}} \leq -F_1 x \leq H_1\Delta[1 \;\; 1]^{\mathrm{T}}. \end{cases} \tag{6.32}$$

The optimal constrained solution in R_8 is given by the normal projection of the unconstrained solution $\tilde{\mathbf{u}}_{\mathrm{UC}}^{\mathrm{OPT}}(x)$ onto face f_4; that is, the solution is obtained by intersecting face f_4 with the normal to it passing through $\tilde{\mathbf{u}}_{\mathrm{UC}}^{\mathrm{OPT}}(x)$. From (6.27) and (6.28), $\tilde{\mathbf{u}}^{\mathrm{OPT}}(x)$ satisfies the equations

$$\begin{aligned} [0 \;\; 1]H^{-1/2}\tilde{\mathbf{u}}^{\mathrm{OPT}}(x) &= \Delta, \\ [1 \;\; 0]H^{1/2}\tilde{\mathbf{u}}^{\mathrm{OPT}}(x) &= [1 \;\; 0]H^{1/2}\tilde{\mathbf{u}}_{\mathrm{UC}}^{\mathrm{OPT}}(x). \end{aligned}$$

Using (6.24) and $\tilde{\mathbf{u}}_{\mathrm{UC}}^{\mathrm{OPT}}(x)$ from (6.25) in the above equations yields

$$H_1 \begin{bmatrix} u_0^{\mathrm{OPT}}(x) \\ \Delta \end{bmatrix} = -F_1 x.$$

Further substitution of $H_1 = \bar{R}[1 + (KB)^2 \;\; KB]$ and $F_1 = \bar{R}(K + KBKA)$ from (6.22) gives

$$u_0^{\rm OPT}(x) = -\frac{(K + KBKA)x + KB\Delta}{1 + (KB)^2},$$

and using the definitions (6.12), we obtain

$$u_0^{\rm OPT}(x) = -Gx - h. \tag{6.33}$$

If we proceed in a similar way with the remaining regions, we obtain a characterisation of the RHC problem (6.2)–(6.7) in the form

$$\mathcal{K}_2(x) = \begin{cases} -Kx & \text{if } x \in R_{\rm UC}, \\ \Delta & \text{if } x \in R_1 \cup R_2 \cup R_3, \\ -Gx + h & \text{if } x \in R_4, \\ -\Delta & \text{if } x \in R_5 \cup R_6 \cup R_7, \\ -Gx - h & \text{if } x \in R_8, \end{cases} \tag{6.34}$$

where

$$\begin{aligned}
R_{\rm UC}: &\quad \begin{cases} |Kx| \le \Delta \\ |K(A-BK)x| \le \Delta \end{cases} \\
R_1: &\quad \begin{cases} -F_1 x \ge H_1 \Delta [1 \;\; 1]^{\rm T} \\ -F_2 x \ge H_2 \Delta [1 \;\; 1]^{\rm T} \end{cases} \\
R_2: &\quad \begin{cases} -Kx \ge \Delta \\ H_2 \Delta [1 \;\; -1]^{\rm T} \le -F_2 x \le H_2 \Delta [1 \;\; 1]^{\rm T} \end{cases} \\
R_3: &\quad \begin{cases} -F_2 x \le H_2 \Delta [1 \;\; -1]^{\rm T} \\ -F_1 x \ge H_1 \Delta [1 \;\; -1]^{\rm T} \end{cases} \\
R_4: &\quad \begin{cases} -K(A-BK)x \le -\Delta \\ H_1 \Delta [-1 \;\; -1]^{\rm T} \le -F_1 x \le H_1 \Delta [1 \;\; -1]^{\rm T} \end{cases} \\
R_5: &\quad \begin{cases} -F_1 x \le H_1 \Delta [-1 \;\; -1]^{\rm T} \\ -F_2 x \le H_2 \Delta [-1 \;\; -1]^{\rm T} \end{cases} \\
R_6: &\quad \begin{cases} -Kx \le -\Delta \\ H_2 \Delta [-1 \;\; -1]^{\rm T} \le -F_2 x \le H_2 \Delta [-1 \;\; 1]^{\rm T} \end{cases} \\
R_7: &\quad \begin{cases} -F_2 x \ge H_2 \Delta [-1 \;\; 1]^{\rm T} \\ -F_1 x \le H_1 \Delta [-1 \;\; 1]^{\rm T} \end{cases}
\end{aligned} \tag{6.35}$$

and R_8 is given in (6.32).

Example 6.4.1. Consider again the system and data of Example 6.2.1. In Figure 6.5 we show the state space partition that corresponds to the controller (6.34)–(6.35) for this example. As can be seen, the RHC law derived

using geometric arguments coincides with the one obtained in Example 6.2.1 by dynamic programming. (Compare with Figure 6.1 (b).) In the following section, we will further discuss this relationship. ∘

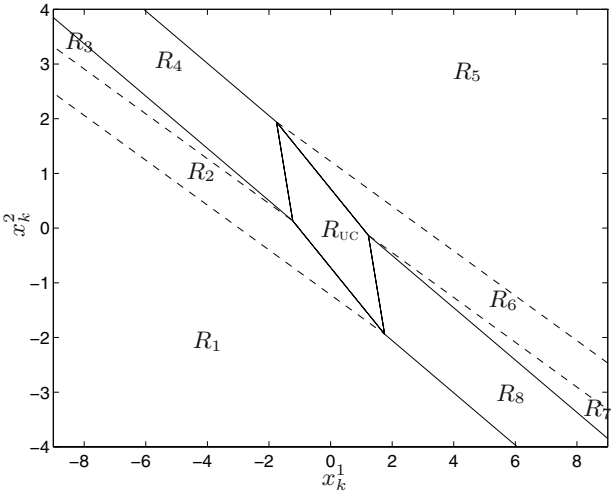

Figure 6.5. State space partitions for Example 6.4.1.

6.4.1 Relationship with the Characterisation Obtained via Dynamic Programming

We will show here that the characterisation (6.11), obtained using dynamic programming, and the characterisation (6.34), obtained using geometric arguments, are equivalent. Indeed, faces f_2 and f_4 of the parallelogram $R_{\rm UC}$ (see Figure 6.6) correspond to the second control u_1 being equal to the saturation limits $-\Delta$ and Δ, respectively. Hence, using the transformation $\mathbf{u} = -H^{-1}Fx$, the definitions of H and F from (6.22), and equating the second component of $\mathbf{u}$ to $-\Delta$ and Δ, we find that these faces are given in the state space by

$$\begin{aligned} f_2: &\qquad -K(A-BK)x = -\Delta, \\ f_4: &\qquad -K(A-BK)x = \Delta. \end{aligned}$$

Comparing the above equations with (6.14), we conclude that region $\mathbb{Z}$ corresponds, in the $\tilde{\mathbf{u}}$-coordinates, to the shaded region in Figure 6.6. Similarly, the half-planes above and below the shaded region in Figure 6.6 correspond to $\mathbb{Z}^-$ and $\mathbb{Z}^+$, defined in (6.13) and (6.15), respectively. Moreover, since faces f_1 and f_3 of the parallelogram $R_{\rm UC}$ (which correspond to the first control u_0 equal to the saturation limits Δ and $-\Delta$, respectively) are given in the state space by

$$f_1: \quad -Kx = \Delta,$$
$$f_3: \quad -Kx = -\Delta,$$

it is not difficult to see, using (6.34), (6.35), that $\mathcal{K}_2(x)$ in $\mathbb{Z}$ is given by $-\text{sat}_\Delta(Kx)$, as stated in (6.11).

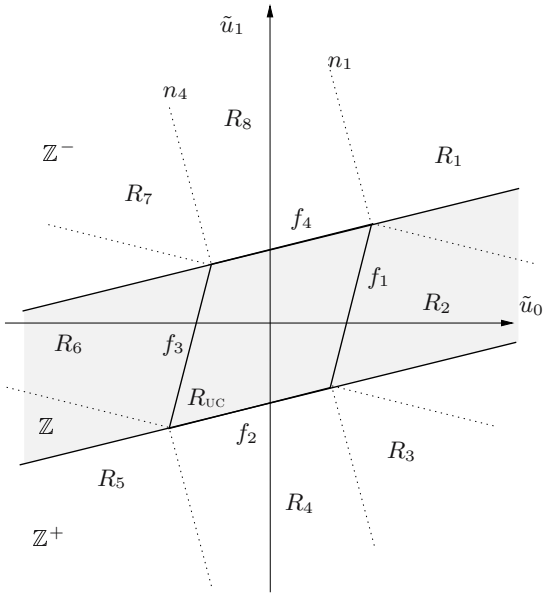

Figure 6.6. Regions that characterise the RHC solution in the case $N = 2$.

On the other hand, substituting (6.26) in (6.29), (6.30), we find that the normals n_1 and n_4 are given in the state space by

$$n_1: \quad -F_1x = H_1 \left[\Delta\ \Delta\right]^{\text{T}},$$
$$n_4: \quad -F_1x = H_1 \left[-\Delta\ \Delta\right]^{\text{T}},$$

and, using $H_1 = \bar{R}[1+(KB)^2 \quad KB]$, $F_1 = \bar{R}(K+KBKA)$, and the definitions (6.12), we have

$$n_1: \quad -Gx - h = \Delta$$
$$n_4: \quad -Gx - h = -\Delta.$$

Thus, comparing with (6.33), we can see that n_1 and n_4 define the switching lines where $\mathcal{K}_2(x) = -Gx - h$ saturates to $\mathcal{K}_2(x) = \Delta$ and $\mathcal{K}_2(x) = -\Delta$, respectively. Then, using (6.34), (6.35), it is immediately seen that $\mathcal{K}_2(x)$ in $\mathbb{Z}^-$ is given by $-\text{sat}_\Delta(Gx + h)$, as stated in (6.11). A similar analysis can be performed for region $\mathbb{Z}^+$.

We have thus far obtained a partition of $\mathbb{R}^2$ that gives a complete geometric picture of the solution to the RHC problem for the case of single input, $N = 2$. One may anticipate that this kind of argument can be extended to larger horizons. This is, indeed, the case, as we will show in Section 6.5, where we will generalise this procedure to higher dimensional spaces.

6.5 Geometric Characterisation for Arbitrary Horizon

In this section we explore the RHC structure for more general problems. We again focus on linear, time-invariant, discrete time models with a quadratic objective function, but we consider arbitrary horizons and more general linear constraints. For these systems, and under a particular constraint qualification, we derive a finitely parameterised characterisation of the RHC solution. In particular, let the system be given by

$$x_{k+1} = Ax_k + Bu_k, \tag{6.36}$$

where $x_k \in \mathbb{R}^n$ and $u_k \in \mathbb{R}^m$. Consider the following fixed horizon optimal control problem:

$$\mathcal{P}_N(x): \qquad V_N^{\mathrm{OPT}}(x) \triangleq \min V_N(\{x_k\}, \{u_k\}), \tag{6.37}$$

subject to:

$$x_{k+1} = Ax_k + Bu_k \quad \text{for } k = 0, \ldots, N-1,$$

$$x_0 = x,$$

$$u_k \in \mathbb{U}_k \quad \text{for } k = 0, \ldots, N-1, \tag{6.38}$$

$$x_k \in \mathbb{X}_k \quad \text{for } k = 0, \ldots, N, \tag{6.39}$$

where $\mathbb{U}_k$ and $\mathbb{X}_k$ are polyhedral constraint sets, whose description we leave unspecified at this stage. The objective function in (6.37) is

$$V_N(\{x_k\}, \{u_k\}) \triangleq \frac{1}{2} x_N^{\mathrm{T}} P x_N + \frac{1}{2} \sum_{k=0}^{N-1} \left(x_k^{\mathrm{T}} Q x_k + u_k^{\mathrm{T}} R u_k \right), \tag{6.40}$$

with $Q > 0$, $R > 0$ and $P \geq 0$.

The associated QP and optimiser are (see (5.29) in Chapter 5)

$$\mathbf{u}^{\mathrm{OPT}}(x) = \arg\min_{L\mathbf{u} \leq W} \frac{1}{2} \mathbf{u}^{\mathrm{T}} H \mathbf{u} + \mathbf{u}^{\mathrm{T}} F x, \tag{6.41}$$

where $\mathbf{u} \in \mathbb{R}^{Nm}$, and where $H = \Gamma^{\mathrm{T}} \mathbf{Q} \Gamma + \mathbf{R}$, $F = \Gamma^{\mathrm{T}} \mathbf{Q} \Omega$, with Γ, Ω, $\mathbf{Q}$, $\mathbf{R}$, defined as in (5.14) and (5.16) of Chapter 5 (with $M = N$ and $C = I$).

The constraint set

$$L\mathbf{u} \leq W \tag{6.42}$$

in (6.41) is a polyhedron in $\mathbb{R}^{Nm}$ obtained from the sets $\mathbb{U}_k$ and $\mathbb{X}_k$ in (6.38) and (6.39), respectively. We will assume that the matrix L and the vector W have the form

$$L = \begin{bmatrix} \Phi \\ -\Phi \end{bmatrix}, \qquad W = \begin{bmatrix} \bar{\Delta} \\ \underline{\Delta} \end{bmatrix} + \begin{bmatrix} -\Lambda \\ \Lambda \end{bmatrix} x. \tag{6.43}$$

In (6.43), Φ is a $q \times Nm$ matrix, $\bar{\Delta}$ and $\underline{\Delta}$ are $q \times 1$ vectors such that $\bar{\Delta} + \underline{\Delta} > 0$ (componentwise), and Λ is a $q \times n$ matrix. Note that (6.42)–(6.43) can also be written as the interval-type constraint $-\underline{\Delta} \leq \Phi \mathbf{u} + \Lambda x \leq \bar{\Delta}$. As was shown in Section 5.3.2 of Chapter 5, the structure of L and W in (6.43) easily accommodates typical constraint requirements, such as, for example, magnitude or rate constraints on the inputs or outputs.

As in Section 6.4, we will study the solution to the above RHC problem using a special coordinate basis for the QP solution space $\mathbb{R}^{Nm}$. To this end, we use the transformation (6.24) to take the original QP coordinates into the new $\tilde{\mathbf{u}}$-coordinates. The convex constraint polyhedron in the $\mathbf{u}$-coordinates defined by (6.42)–(6.43), is mapped into a convex constraint polyhedron in the $\tilde{\mathbf{u}}$-coordinates, given by

$$\tilde{\Phi}\tilde{\mathbf{u}} \leq \bar{\Delta} - \Lambda x, \tag{6.44}$$

$$-\tilde{\Phi}\tilde{\mathbf{u}} \leq \underline{\Delta} + \Lambda x, \tag{6.45}$$

where

$$\tilde{\Phi} \triangleq \Phi H^{-1/2}.$$

Notice that the dimension of the constraint polyhedron is the constraint horizon $q = \text{rank } \Phi$. A *face* of the constraint polyhedron is defined by the intersection, with the constraint polyhedron, of the hyperplane defined by a subset of equalities (or active constraints) within (6.44)–(6.45). To each face of the constraint polyhedron, we will associate an *active pair* (ℓ, Δ), whose elements are defined below. We will use the notation 6.4.1, and introduce the set $J \triangleq \{1, 2, \ldots, q\}$ of the first q natural numbers. We then define, for each face with $\bar{N} \in J$ active constraints:

- The *active set* $\ell \triangleq \{\ell_1, \ell_2, \ldots, \ell_{\bar{N}} : \ell_k \in J\}$, which identifies the indices of the constraints that are active; that is, the indices of the rows within (6.44)–(6.45) that hold as equalities for the face. Note that the gradient of the active constraints is $\tilde{\Phi}_\ell$.
- The *active value vector* $\Delta \in \mathbb{R}^{\bar{N}}$, which identifies whether the active constraint whose index is ℓ_k corresponds to either row ℓ_k of (6.44) or row ℓ_k of (6.45). More precisely, the kth element of Δ is given by

$$\begin{cases} \Delta_k = \bar{\Delta}_{\ell_k} & \text{if } \tilde{\Phi}_{\ell_k}\tilde{\mathbf{u}} = \bar{\Delta}_{\ell_k} - \Lambda_{\ell_k} x, \\ \Delta_k = -\underline{\Delta}_{\ell_k} & \text{if } \tilde{\Phi}_{\ell_k}\tilde{\mathbf{u}} = -\underline{\Delta}_{\ell_k} - \Lambda_{\ell_k} x. \end{cases} \tag{6.46}$$

- The *inactive set* $s \triangleq J - \ell = \{s_1, s_2, \ldots, s_{q-\bar{N}} : s_k \in J \text{ and } s_k \notin \ell\}$, which identifies the indices of the constraints that are not active in each face. Note that the gradient of the inactive constraints is $\tilde{\Phi}_s$.

In addition, we will impose the *constraint qualification* that the gradient of active constraints $\tilde{\Phi}_\ell$ has full row rank.

Each active pair (ℓ, Δ) fully characterises an *active face* of the constraint polyhedron, which is given by the intersection with the constraint polyhedron of the hyperplane defined by the equality constraint

$$\tilde{\Phi}_\ell \tilde{\mathbf{u}} = \Delta - \Lambda_\ell x. \tag{6.47}$$

For example, in Figure 6.7, (6.47) may represent the plane that contains face f_1, in which case one constraint is active, or the line that contains e_1, in which case two constraints are active.

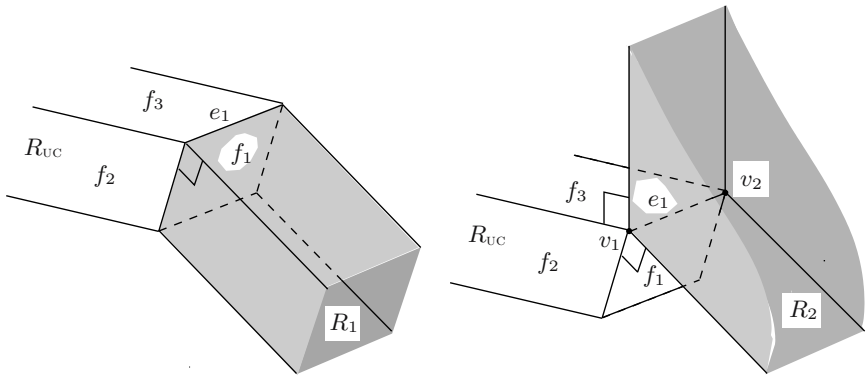

(a) Active region associated with a face.

(b) Active region associated with an edge.

Figure 6.7. Illustration of active regions associated with a face and an edge of the constraint polyhedron.

To each active face, we will then associate an *active region* of $\mathbb{R}^{Nm}$ defined as the set of all points $v \in \mathbb{R}^{Nm}$ for which the point of the constraint polyhedron that is closest to v, in Euclidean distance, belongs to the corresponding active face. For example, region R_1 in Figure 6.7 (a) is an active region associated with face f_1 and region R_2 in Figure 6.7 (b) is an active region associated with edge e_1. In these regions, the optimal solution $\tilde{\mathbf{u}}^{\text{OPT}}(x)$ is simply given by the point on the corresponding active face of the constraint polyhedron that is closest, in the Euclidean distance, to the unconstrained solution $\tilde{\mathbf{u}}^{\text{OPT}}_{\text{UC}}(x) = -H^{-1/2}Fx$ (see, for example, Figure 6.4).

The following lemma characterises, for an arbitrary active pair (ℓ, Δ), the corresponding active region in $\mathbb{R}^{Nm}$.

Lemma 6.5.1 (Active Regions) *Suppose that the gradient of active constraints $\tilde{\Phi}_\ell$ has full row rank. Then the active region corresponding to the face characterised by the equality constraint* (6.47) *is given by*

$$S\left\{[\tilde{\Phi}_\ell\tilde{\Phi}_\ell^{\mathrm{T}}]^{-1}[\tilde{\Phi}_\ell\tilde{\mathbf{u}}+\Lambda_\ell x-\Delta]\right\}\leq 0, \tag{6.48}$$

$$-\underline{\Delta}_s\leq\tilde{\Phi}_s\tilde{\mathbf{u}}+\Lambda_s x-\tilde{\Phi}_s\tilde{\Phi}_\ell^{\mathrm{T}}[\tilde{\Phi}_\ell\tilde{\Phi}_\ell^{\mathrm{T}}]^{-1}[\tilde{\Phi}_\ell\tilde{\mathbf{u}}+\Lambda_\ell x-\Delta]\leq\bar{\Delta}_s, \tag{6.49}$$

where Δ *is defined in* (6.46) *and* S *is a sign diagonal matrix such that its* (k,k)*-entry is* $S_{kk}=1$ *if* $\Delta_k=-\underline{\Delta}_{\ell_k}$ *and* $S_{kk}=-1$ *if* $\Delta_k=\bar{\Delta}_{\ell_k}$.

Proof. Geometrically, the active region corresponding to the face characterised by the active constraints (6.47) is delimited by[1]:

- *Each hyperplane that contains the corresponding active face* (6.47) *and is normal to one of the faces that share with the active face all but one of its active constraints.* (For example, in Figure 6.7 (b), these hyperplanes are the two planes delimiting R_2 that are normal to faces f_1 and f_3 and contain edge e_1.)

  We will show that these hyperplanes are given by the equality in each row of (6.48). First, it is easy to see that these equalities contain (6.47) simply by substitution of (6.47) in (6.48). Next, note that each face that shares with (6.47) all the active constraints except constraint ℓ_k is characterised by the equality constraint

  $$\tilde{\Phi}_{\ell-\ell_k}\tilde{\mathbf{u}}=\Delta'-\Lambda_{\ell-\ell_k}x, \tag{6.50}$$

  where Δ' is formed from Δ by eliminating its kth element. We now rewrite the equality in (6.48) as

  $$\Psi\tilde{\mathbf{u}}=[\tilde{\Phi}_\ell\tilde{\Phi}_\ell^{\mathrm{T}}]^{-1}[-\Lambda_\ell x+\Delta] \tag{6.51}$$

  where $\Psi\triangleq[\tilde{\Phi}_\ell\tilde{\Phi}_\ell^{\mathrm{T}}]^{-1}\tilde{\Phi}_\ell$. Since $\Psi\tilde{\Phi}_\ell^{\mathrm{T}}=I$, it follows that $\Psi_k\tilde{\Phi}_{\ell-\ell_k}=0_{1\times(\bar{N}-1)}$. Hence, the hyperplane defined by the kth row of (6.51) is normal to the face (6.50), as claimed. Note that this holds for $k=1,\ldots,\bar{N}$, which covers all rows of (6.48).

- *Each hyperplane that is normal to the corresponding active face* (6.47) *and contains one of the faces that share with the active face all its active constraints and has one more active constraint.* (For example, in Figure 6.7 (b), these hyperplanes are the two parallel planes delimiting R_2 that are normal to e_1 and contain vertices v_1 and v_2.)

  We will show that these hyperplanes are given by the equalities in each row of (6.49). The matrix multiplying $\tilde{\mathbf{u}}$ in (6.49), $\tilde{\Phi}_s[I-\tilde{\Phi}_\ell^{\mathrm{T}}[\tilde{\Phi}_\ell\tilde{\Phi}_\ell^{\mathrm{T}}]^{-1}\tilde{\Phi}_\ell]$, satisfies

  $$\tilde{\Phi}_s[I-\tilde{\Phi}_\ell^{\mathrm{T}}[\tilde{\Phi}_\ell\tilde{\Phi}_\ell^{\mathrm{T}}]^{-1}\tilde{\Phi}_\ell]\tilde{\Phi}_\ell^{\mathrm{T}}=\tilde{\Phi}_s[\tilde{\Phi}_\ell^{\mathrm{T}}-\tilde{\Phi}_\ell^{\mathrm{T}}I]=0, \tag{6.52}$$

  and hence each equality in (6.49) is normal to the active face (6.47). Next, note that each face that shares with the active face (6.47) all its active

[1] See, for example, region R_2 in Figure 6.7 (b), corresponding to the edge e_1.

constraints and has one more active constraint, s_k, say, satisfies both (6.47) and an additional constraint of the form

$$\tilde{\Phi}_{s_k}\tilde{\mathbf{u}} = \bar{\Delta}_{s_k} - \Lambda_{s_k}x, \tag{6.53}$$

or of the same form with $-\underline{\Delta}_{s_k}$ replacing $\bar{\Delta}_{s_k}$. Then, substituting (6.47) and (6.53) in (6.49) it is easy to see that the kth row satisfies the right equality constraint. Thus, the hyperplane defined by the kth row of the right equality in (6.49) contains the face that is characterised by the equality constraints (6.47) and (6.53). A similar analysis can be done for the left equality constraint. Note that this holds for $k = 1, \ldots, q - \bar{N}$, which covers all rows of (6.49). The result then follows.

□

For each active region characterised in Lemma 6.5.1 we can then compute the optimal solution $\tilde{\mathbf{u}}^{\mathrm{OPT}}(x)$ of the QP (6.41) as the point on the corresponding active face of the constraint polyhedron that is closest, in the Euclidean distance, to the unconstrained solution $\tilde{\mathbf{u}}^{\mathrm{OPT}}_{\mathrm{UC}}(x) = -H^{-1/2}Fx$. Also, to each active region characterised in Lemma 6.5.1 the transformation (6.26) assigns a corresponding region in the state space. The following theorem summarises this procedure by characterising for an arbitrary active pair (ℓ, Δ) the corresponding active region in the state space and the corresponding optimal solution of the QP (6.41) with constraints given by (6.42)–(6.43).

Theorem 6.5.2 (QP Solution in an Active Region) *Under the conditions of Lemma 6.5.1, the projection X_ℓ onto the state space of the active region defined by* (6.48)–(6.49) *is given by*

$$\begin{aligned} S\left\{[\tilde{\Phi}_\ell\tilde{\Phi}_\ell^{\mathrm{T}}]^{-1}[(-\tilde{\Phi}_\ell H^{-1/2}F + \Lambda_\ell)x - \Delta]\right\} &\leq 0, \\ -\tilde{\Phi}_s H^{-1/2}Fx + \Lambda_s x - \tilde{\Phi}_s\tilde{\Phi}_\ell^{\mathrm{T}}[\tilde{\Phi}_\ell\tilde{\Phi}_\ell^{\mathrm{T}}]^{-1}[-\tilde{\Phi}_\ell H^{-1/2}Fx + \Lambda_\ell x - \Delta] &\leq \bar{\Delta}_s, \\ \tilde{\Phi}_s H^{-1/2}Fx - \Lambda_s x + \tilde{\Phi}_s\tilde{\Phi}_\ell^{\mathrm{T}}[\tilde{\Phi}_\ell\tilde{\Phi}_\ell^{\mathrm{T}}]^{-1}[-\tilde{\Phi}_\ell H^{-1/2}Fx + \Lambda_\ell x - \Delta] &\leq \underline{\Delta}_s. \end{aligned} \tag{6.54}$$

Moreover, if $x \in X_\ell$, the optimal constrained control $\mathbf{u}^{\mathrm{OPT}}(x)$ in (6.41) *is given by*

$$\mathbf{u}^{\mathrm{OPT}}(x) = H^{-1/2}\tilde{\Phi}_\ell^{\mathrm{T}}[\tilde{\Phi}_\ell\tilde{\Phi}_\ell^{\mathrm{T}}]^{-1}(\Delta - \Lambda_\ell x) - H^{-1/2}[I - \tilde{\Phi}_\ell^{\mathrm{T}}[\tilde{\Phi}_\ell\tilde{\Phi}_\ell^{\mathrm{T}}]^{-1}\tilde{\Phi}_\ell]H^{-1/2}Fx. \tag{6.55}$$

Proof. Equations (6.54) follow immediately upon substitution of (6.26) into (6.48) and (6.49). We now show that the optimal control inside each region (6.54) has the form (6.55). Indeed, the optimal constrained control in each of the active regions is obtained by intersecting the active face (6.47) with the hyperplane normal to it and passing through the unconstrained solution $\tilde{\mathbf{u}}^{\mathrm{OPT}}_{\mathrm{UC}}(x)$. That is, $\tilde{\mathbf{u}}^{\mathrm{OPT}}(x)$ satisfies both (6.47) and the following equation (see (6.52)):

$$[I - \tilde{\Phi}_\ell^{\mathrm{T}}[\tilde{\Phi}_\ell\tilde{\Phi}_\ell^{\mathrm{T}}]^{-1}\tilde{\Phi}_\ell]\tilde{\mathbf{u}}^{\mathrm{OPT}}(x) = [I - \tilde{\Phi}_\ell^{\mathrm{T}}[\tilde{\Phi}_\ell\tilde{\Phi}_\ell^{\mathrm{T}}]^{-1}\tilde{\Phi}_\ell]\tilde{\mathbf{u}}_{\mathrm{UC}}^{\mathrm{OPT}}(x).$$

Substituting (6.47) and $\tilde{\mathbf{u}}_{\mathrm{UC}}^{\mathrm{OPT}}(x) = -H^{-1/2}Fx$ from (6.25) into the above equation, and solving for $\tilde{\mathbf{u}}^{\mathrm{OPT}}(x)$, yields

$$\tilde{\mathbf{u}}^{\mathrm{OPT}}(x) = \tilde{\Phi}_\ell^{\mathrm{T}}[\tilde{\Phi}_\ell\tilde{\Phi}_\ell^{\mathrm{T}}]^{-1}(\Delta - \Lambda_\ell x) - [I - \tilde{\Phi}_\ell^{\mathrm{T}}[\tilde{\Phi}_\ell\tilde{\Phi}_\ell^{\mathrm{T}}]^{-1}\tilde{\Phi}_\ell]H^{-1/2}Fx. \quad (6.56)$$

Equation (6.55) follows using the transformation (6.24). The theorem is then proved. □

Theorem 6.5.2 gives the solution of the QP (6.41) if x belongs to the region X_ℓ defined by (6.54). The RHC law $\mathcal{K}_N(x) = u_0^{\mathrm{OPT}}(x)$ is then simply obtained by selecting the first m elements of $\mathbf{u}^{\mathrm{OPT}}(x)$ in (6.55), that is,

$$\mathcal{K}_N(x) = u_0^{\mathrm{OPT}}(x) = \begin{bmatrix} I & 0 & \cdots & 0 \end{bmatrix} \mathbf{u}^{\mathrm{OPT}}(x). \quad (6.57)$$

To obtain the complete solution in the state space, one would require a procedure to enumerate all possible combinations of active constraints and compute the corresponding region and optimal control for each combination using Theorem 6.5.2. An algorithm that implements such a procedure is described in Seron, Goodwin and De Doná (2003). We observe that, if the state space dimension n is $n < Nm$, then the image of the transformation $\mathbf{u}_{\mathrm{UC}}^{\mathrm{OPT}}(x) = -H^{-1}Fx$ is a lower dimensional subspace of $\mathbb{R}^{Nm}$, and so some of the regions X_ℓ in (6.54) will be empty. Hence, the partition has to be post-processed to eliminate redundant inequalities and empty regions. If $n \geq Nm$, then the computation of the region partition using Theorem 6.5.2 combined with the enumeration of all possible combinations of active constraints directly gives the complete state space partition with no need for further processing.

We illustrate the procedure with a numerical example.

Example 6.5.1. Consider a system of the form (6.36) with matrices

$$A = \begin{bmatrix} 0.8955 & -0.1897 \\ 0.0948 & 0.9903 \end{bmatrix}, \qquad B = \begin{bmatrix} 0.0948 \\ 0.0048 \end{bmatrix}.$$

In the objective function (6.40) we take $N = 4$, $Q = \begin{bmatrix} 0 & 0 \\ 0 & 2 \end{bmatrix}$ and $R = 0.01$. The terminal state weighting matrix P is chosen as the solution of the algebraic Riccati equation $P = A^{\mathrm{T}}PA + Q - K^{\mathrm{T}}\bar{R}K$, where $K \triangleq \bar{R}^{-1}B^{\mathrm{T}}PA$ and $\bar{R} \triangleq R + B^{\mathrm{T}}PB$. We consider constraints of the form (6.42), with $m = 1$, $N = 4$, $\Phi = I$, $\Lambda = 0_{Nm\times n}$, and $\Delta = \begin{bmatrix} 2 & 2 & 2 & 2 \end{bmatrix}^{\mathrm{T}}$.

The state space partition for this case, computed using Theorem 6.5.2 and the enumeration algorithm of Seron et al. (2003), is shown in Figure 6.8 (a). A "zoom" of this partition is shown in Figure 6.8 (b) to display the smaller regions in more detail. The region denoted by X_0 is the projection onto the state space of the constraint polyhedron; in regions X_2, X_3 and X_4 only one constraint is active; in regions X_5 and X_6 two constraints are active; in region

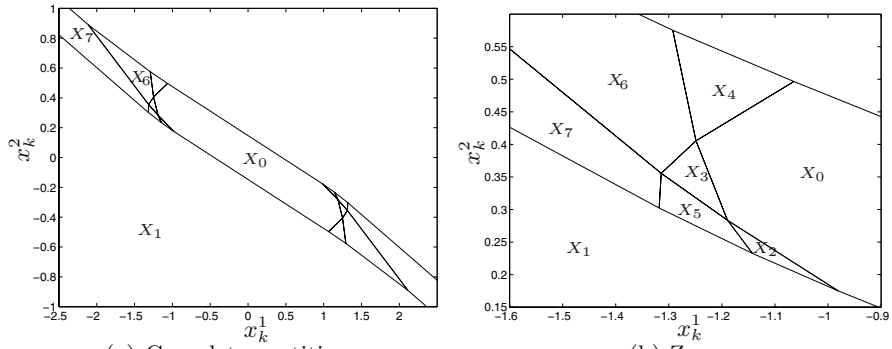

(a) Complete partition. (b) Zoom.

Figure 6.8. State space partition for Example 6.5.1 for $N = 4$.

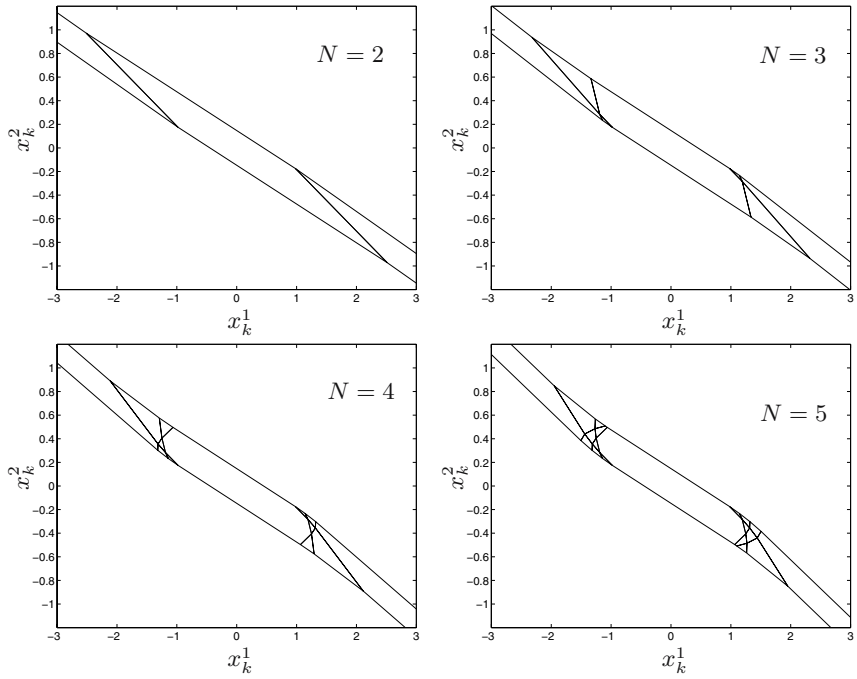

Figure 6.9. State space partition for Example 6.5.1 for $N = 2, 3, 4, 5$.

X_7 three constraints are active; finally, X_1 is the union of all regions where the control is saturated to the value -2.

The resulting RHC law (6.57) is

$$\mathcal{K}_4(x) = G_i x + h_i, \quad \text{if } x \in X_i, \quad i = 0, \ldots, 7, \tag{6.58}$$

where

$$
\begin{aligned}
G_0 &= -[4.4650 \quad 13.5974], & h_0 &= 0,\\
G_1 &= \begin{bmatrix} 0 & 0 \end{bmatrix}, & h_1 &= -2,\\
G_2 &= -[5.6901 \quad 15.9529], & h_2 &= -0.7894,\\
G_3 &= -[4.9226 \quad 13.8202], & h_3 &= -0.4811,\\
G_4 &= -[4.5946 \quad 13.3346], & h_4 &= -0.2684,\\
G_5 &= -[6.6778 \quad 16.8644], & h_5 &= -1.7057,\\
G_6 &= -[5.1778 \quad 13.4855], & h_6 &= -0.9355,\\
G_7 &= -[7.4034 \quad 16.8111], & h_7 &= -2.6783.
\end{aligned}
$$

Similar expressions hold in the remaining unlabelled regions. These can be obtained by symmetry.

To see how the partitions are affected by the constraint horizon, we take, successively, $N = 2$, $N = 3$, $N = 4$ and $N = 5$ in the objective function (6.40). The state space partitions corresponding to each value of N are shown in Figure 6.9.

We next consider an initial condition $x_0 = [-1.2 \;\; 0.53]^{\mathrm{T}}$ and simulate the system under the RHC (6.58). Figure 6.10 shows the resulting state space trajectory. The trajectory starts in region X_4 and moves, successively, into regions X_6, X_5, X_1, X_1, X_0, and stays in X_0 thereafter. Table 6.1 shows the trajectory points x_k for $k = 0, \ldots, 6$, the regions X_i such that $x_k \in X_i$, and the corresponding RHC controls computed using (6.58). ∘

k	x_k	Region X_i	RHC control u_k
0	$[-1.2000 \quad 0.5300]^{\mathrm{T}}$	X_4	$-[4.5946 \quad 13.3346]x_k - 0.2684$
1	$[-1.3480 \quad 0.4023]^{\mathrm{T}}$	X_6	$-[5.1778 \quad 13.4855]x_k - 0.9355$
2	$[-1.2247 \quad 0.2735]^{\mathrm{T}}$	X_5	$-[6.6778 \quad 16.8644]x_k - 1.7057$
3	$[-0.9722 \quad 0.1637]^{\mathrm{T}}$	X_1	$[0 \quad 0]x_k - 2.0000$
4	$[-0.7120 \quad 0.0796]^{\mathrm{T}}$	X_1	$[0 \quad 0]x_k - 2.0000$
5	$[-0.4630 \quad 0.0209]^{\mathrm{T}}$	X_0	$-[4.4650 \quad 13.5974]x_k$
6	$-[0.2495 \quad 0.0146]^{\mathrm{T}}$	X_0	$-[4.4650 \quad 13.5974]x_k$
⋮	⋮	⋮	⋮

Table 6.1. Example 6.5.1: Trajectory x_k, $k = 0, \ldots, 6$, regions X_i such that $x_k \in X_i$, and corresponding RHC controls (6.58).

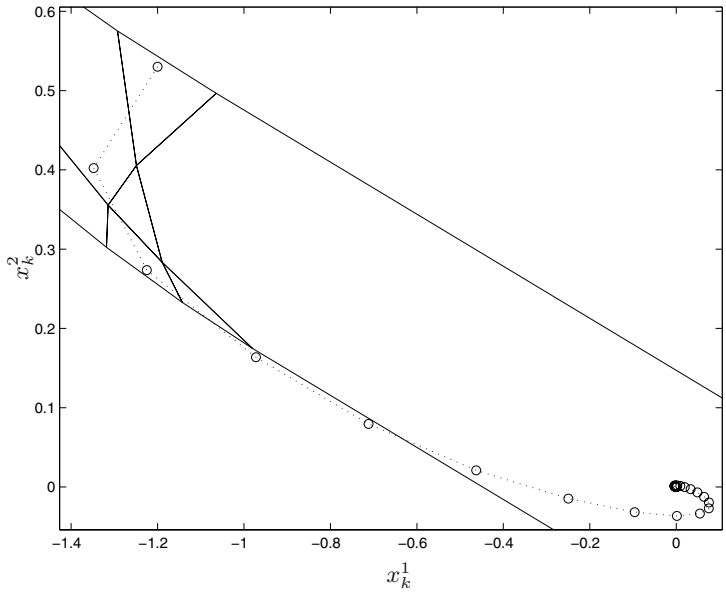

Figure 6.10. State space trajectory for Example 6.5.1 with $N = 4$, $x_0 = [-1.2 \;\; 0.53]^{\mathrm{T}}$.

6.6 Characterisation Using the KKT Conditions

The parameterisation given in Theorem 6.5.2 can be related to the KKT optimality conditions studied in Chapter 2. Consider again the QP (6.41) with constraints given by (6.42)–(6.43). For convenience, we will work in the $\tilde{\mathbf{u}}$-coordinates given by the transformation (6.24), that is, we consider the following QP with inequality constraints:

$$\begin{aligned} &\text{minimise } \frac{1}{2}\tilde{\mathbf{u}}^{\mathrm{T}}\tilde{\mathbf{u}} + \tilde{\mathbf{u}}^{\mathrm{T}}H^{-1/2}Fx, \\ &\text{subject to:} \\ &\tilde{\Phi}\tilde{\mathbf{u}} \leq \bar{\Delta} - \Lambda x, \\ &-\tilde{\Phi}\tilde{\mathbf{u}} \leq \underline{\Delta} + \Lambda x. \end{aligned} \tag{6.59}$$

When solved for different values of x, the above problem is sometimes referred to as a *multiparametric quadratic program* [mp-QP], that is, a QP in which the linear term in the objective function and the right hand side of the constraints depend linearly on a vector of parameters (the state vector x in this case).

Let $\tilde{\mathbf{u}}^{\mathrm{OPT}}(x)$ be the optimal solution of (6.59). As discussed in Section 2.5.6 of Chapter 2, the KKT optimality conditions are both necessary and sufficient conditions for this problem. Using (2.41) of Chapter 2, we can write the KKT conditions for the above problem as

$$-\underline{\Delta} \leq \tilde{\Phi}\tilde{\mathbf{u}}^{\mathrm{OPT}}(x) + \Lambda x \leq \bar{\Delta}, \tag{6.60}$$

$$\tilde{\mathbf{u}}^{\mathrm{OPT}}(x) + H^{-1/2}Fx + \tilde{\Phi}^{\mathrm{T}}(\mu - \sigma) = 0, \tag{6.61}$$

$$\mu \geq 0, \qquad \sigma \geq 0, \tag{6.62}$$

$$\mu^{\mathrm{T}}[\tilde{\Phi}\tilde{\mathbf{u}}^{\mathrm{OPT}}(x) - \bar{\Delta} + \Lambda x] = 0, \tag{6.63}$$

$$\sigma^{\mathrm{T}}[\tilde{\Phi}\tilde{\mathbf{u}}^{\mathrm{OPT}}(x) + \underline{\Delta} + \Lambda x] = 0, \tag{6.64}$$

where $\mu \in \mathbb{R}^q$ and $\sigma \in \mathbb{R}^q$ are vectors of Lagrange multipliers corresponding to the two sets of inequality constraints in (6.59).

Consider now an active pair (ℓ, Δ) for $\tilde{\mathbf{u}}^{\mathrm{OPT}}(x)$, where Δ satisfies (6.46), and let s be the corresponding inactive set. We then have that $\tilde{\mathbf{u}}^{\mathrm{OPT}}(x)$ satisfies the equality constraints (6.47), that is,

$$\tilde{\Phi}_\ell \tilde{\mathbf{u}}^{\mathrm{OPT}}(x) = \Delta - \Lambda_\ell x. \tag{6.65}$$

From the above equation, the complementary slackness conditions (6.63) and (6.64), the (second) dual feasibility condition (6.62), and equation (6.46), we have that

$$\mu_s = 0, \qquad \sigma_s = 0, \tag{6.66}$$

$$\mu_{\ell_k} - \sigma_{\ell_k} \begin{cases} \geq 0 & \text{if } \Delta_k = \bar{\Delta}_{\ell_k}, \\ \leq 0 & \text{if } \Delta_k = -\underline{\Delta}_{\ell_k}. \end{cases} \tag{6.67}$$

Using (6.66) in the (first) dual feasibility condition (6.61) and solving for $\tilde{\mathbf{u}}^{\mathrm{OPT}}(x)$ yields

$$\tilde{\mathbf{u}}^{\mathrm{OPT}}(x) = -H^{-1/2}Fx - \tilde{\Phi}_\ell^{\mathrm{T}}[\mu_\ell - \sigma_\ell]. \tag{6.68}$$

Using (6.68) in the active constraint equality (6.65) and solving for $[\mu_\ell - \sigma_\ell]$ gives

$$[\mu_\ell - \sigma_\ell] = [\tilde{\Phi}_\ell \tilde{\Phi}_\ell^{\mathrm{T}}]^{-1}[-\tilde{\Phi}_\ell H^{-1/2}Fx + \Lambda_\ell x - \Delta]. \tag{6.69}$$

Substituting the above equation into (6.68) we obtain

$$\tilde{\mathbf{u}}^{\mathrm{OPT}}(x) = \tilde{\Phi}_\ell^{\mathrm{T}}[\tilde{\Phi}_\ell \tilde{\Phi}_\ell^{\mathrm{T}}]^{-1}(\Delta - \Lambda_\ell x) - [I - \tilde{\Phi}_\ell^{\mathrm{T}}[\tilde{\Phi}_\ell \tilde{\Phi}_\ell^{\mathrm{T}}]^{-1}\tilde{\Phi}_\ell]H^{-1/2}Fx, \tag{6.70}$$

which is identical to (6.56). We then recover the expression (6.55) for the optimal solution using the transformation (6.24).

The inequalities (6.54) that define the region in the state space where the optimal solution (6.55) is valid can be recovered in the following way: Combining the expression for the difference of Lagrange multipliers (6.69) and the sign condition (6.67) yields the first set of inequalities in (6.54) (recall that S is a sign diagonal matrix such that $S_{kk} = 1$ if $\Delta_k = -\underline{\Delta}_{\ell_k}$ and $S_{kk} = -1$ if $\Delta_k = \bar{\Delta}_{\ell_k}$). Finally, the second and third sets of inequalities in (6.54) follow from primal feasibility (see (6.60)) of the inactive constraints, that is,

$$-\underline{\Delta}_s \leq \tilde{\Phi}_s \tilde{\mathbf{u}}^{\mathrm{OPT}}(x) + \Lambda_s x \leq \bar{\Delta}_s,$$

upon substitution of the expression (6.70) for the optimal solution.

In summary, we can see that the characterisation of Theorem 6.5.2 is a particular arrangement of the KKT optimality conditions.

6.7 Further Reading

For complete list of references cited, see References section at the end of book.

General

The global characterisation presented here is based on the work of Bemporad et al. (2002) and Seron et al. (2003).

Section 6.5

A related development to the one presented in Section 6.5 is described in Seron et al. (2003).

Section 6.6

The approach described in Section 6.6 using KKT conditions was used in Bemporad et al. (2002) to obtain a local characterisation of the QP solution in an active region of the state space around a specific solution $\tilde{\mathbf{u}}^{\mathrm{OPT}}(x)$. In that work, once a nonempty active region has been defined, the rest of the state space is explored in the search for new active regions.

In the above context, an algorithm to explore and partition the rest of the state space in polyhedral regions was originally proposed in Dua and Pistikopoulos (2000). This algorithm recursively reverses the inequalities that define each active region to obtain a new region partition. In each new region of the resulting partition a feasible point x is found (possibly by solving a linear program). Then, a QP of the form (6.59) is solved for that value of x to determine the active constraints that characterise the active region using the KKT conditions as described above. One drawback of this algorithm is that it can split active regions since the regions to be explored are not necessarily related to the active regions.

A more efficient algorithm to accomplish the state space partitioning was proposed by Tøndel, Johansen and Bemporad (2002). The main contribution of this algorithm is that the active constraints in the region of interest can be determined from the active constraints in a neighbouring region by examining the separating hyperplane between these regions. Thus, QPs do not need to be solved to determine the active set of constraints in each region and, moreover, unnecessary partitioning is avoided.